Influence of Variable Swirl on Emissions in a Non-Premixed Fuel-Flexible Burner at Elevated Ambient Conditions

Daniel Pugh
Cardiff University
Cardiff, UK

Phil Bowen
Cardiff University
Cardiff, UK

Rukshan Navaratne
Cardiff University
Cardiff, UK

Burak Goktepe
Cardiff University
Cardiff, UK

Anthony Giles
Cardiff University
Cardiff, UK

Agustin Valera Medina
Cardiff University
Cardiff, UK

Steven Morris
Cardiff University
Cardiff, UK

Robin Vivoli
Cardiff University
Cardiff, UK

ABSTRACT

As alternative fuels are designated for future energy applications, flexible combustor designs require considerable development to ensure stable operation with reduced NOx emissions. A non-premixed variable swirl burner was used to experimentally appraise changes in NO production pathways, with CH_4 NH_3, and H_2 flames, alongside intermediate fuel blends. Maintaining an equivalent thermal power and flame temperature between fuels, preheated reactants (500 K) were supplied to the burner, with parametric changes made to pressure (1 - 6 bar_a) and swirl number (0.8 - 2.0). NO production was characterized, alongside variations in flame structure and topology, with a correlation demonstrated for exhaust emissions. NO production was shown to be sensitive to combustor pressure, providing an expected increase for CH_4 and H_2 flames. Emission profiles from both NH_3 and H_2 flames are shown to be significantly augmented by a change in swirl number. As NH_3 fractions were increased in the H_2 blend, a decaying trend in NO emissions was observed with an increase in pressure, and as a function of mixture ratio. However, this behaviour was markedly augmented by a change in swirl number and suggests that further reductions may be possible at increased pressure. At the low swirl/high pressure condition the NH_3/H_2 blend outperformed pure H_2, providing lower NO concentrations. Emissions data were normalised using the traditional dry/O_2 correction, alongside mass scaled by thermal power, with a comparison provided. The corresponding differences in emission formation pathways were investigated, alongside high-speed OH chemiluminescence to further elucidate findings.*

Keywords: Hydrogen, Combustion, Low-emission combustor, Turbulence, Fuel combustion.

NOMENCLATURE

A_{noz}	Area of the burner nozzle exit
A_{tan}	Tangential inlet area
AFT	Adiabatic flame temperature
$\dot{m}_x$	Mass flow rate of x
P	Burner ambient pressure
q_{in}	Thermal input power
Q_{tan}	Tangential flow rate
Q_{total}	Total flow rate
r_{noz}	Burner nozzle radius
r_{tan}	Effective radius of the tangential inlet
Re	Reynolds number
Sg	Geometric swirl number
T	Burner inlet temperature
$\dot{V}_x$	Volumetric flow of x
X_x	Mole fraction of x
ρ_x	Mass density of x
Φ	Global fuel-air equivalence ratio

1. INTRODUCTION

Future energy transfer applications will require the use of alternative fuels to achieve evolving emissions targets, comprising a range of technologies to meet the differences between fluctuating renewable supply and transient demand. From the perspective of anthropogenic climate change, significant emissions from fossil fuels include carbon dioxide (CO_2) and methane (CH_4), alongside Nitrous oxide (N_2O), with the latter possessing a 100-year global warming of potential (GWP) ~265 times that of CO_2 [1]. This is noteworthy, as even with the development and application of alternative, carbon-free fuels such as Hydrogen (H_2) and Ammonia (NH_3), the production of all emissions must be suitably quantified to facilitate the development of flexible, efficient, and non-

polluting combustion systems. This includes more traditional concern for formation of Nitrogen Oxides (NO_x, typically NO and NO_2), which can also provide detrimental impacts on both respiratory health and the environment. Whilst NO_x emissions were already a primary consideration for natural gas fired systems, this concern will continue to develop with the challenging application of carbon-free alternative fuels. A range of combustor configurations can be employed for optimized emissions production, such as the lean premixed dry low emission (DLE) strategy. However, fuel-flexible operation remains a challenge, with associated stability issues such as flashback [2]. Non-premixed combustors can offer advantages in relation to flame stability, however often at the expense of emissions performance. The aim of the research presented herein is to appraise experimentally the relative emissions performance of a fuel-flexible combustor at elevated conditions of temperature and pressure, with changing burner geometry.

1.1 Research Scope

The configuration employed comprised a turbulent fuel jet, with co-annular swirling airflow, housed inside an optical pressure casing. Three fuels (CH_4, H_2, and NH_3) were applied both independently and in different mixture ratios, with the influence of fuel-air turbulent mixing appraised using a variation in geometric swirl number (defined in section 2.1) alongside an increase in inlet ambient pressure. Numerous studies have demonstrated the complex potential influence of varying swirl number on emissions formation for both CH_4 [3, 4] and H_2 [5] with non-premixed flames. Kim et al. [6] investigated the influence of CH_4/H_2 blends and demonstrated an increase in local temperature and NO_x with H_2 addition, offset by a reduction for increasing swirl intensity. Results were also compared between premixed and diffusion configurations, with the latter providing lower emissions. Results from Gupta et al. [7] also suggested a sensitivity for NO_x emissions to change with swirl in a premixed CH_4 flame. Kashir et al. [8] demonstrated numerically a reduction in flame length with both increasing swirl and H_2 addition in a non-premixed CH_4 flame, whereas De and Acharya [9] showed greater swirl broadens the size of recirculation zone for a fixed H_2 enriched mixture. The numerical work of Ilbas et al. [10] predicted an increase in NO_x with swirl for H_2 enriched fuels due to changing temperature gradients. The influence of swirl strength has also been demonstrated in alternative combustor architectures. Khalil and Gupta [11] investigated swirl in a distributed CH_4 combustor and observed that higher residence times and stronger swirl generates greater combustion efficiency, whilst providing lower levels of NO and CO. Patel and Shah [12] compared swirling and non-swirling inverse diffusion flames and observed an increase in NO_x with H_2, and more prominent in the case of non-swirling flow.

Experimental data are more limited in the context of fuel switching for turbine relevant conditions, particularly for NH_3. However, more data are available for trends observed with other alternative fuels. Jalalatian [13] investigated the influence of swirl and equivalence ratio on emissions for bluff-body stabilized Propane (C_3H_8) flames and found a change in sensitivity relative to Reynolds number with increasing swirl. Mansouri et al [14] saw a significant reduction in CO emissions with increased swirl from H_2 enriched C_3H_8 flames. Chiong et al [15] demonstrated a reduction in NO emissions with an increase in swirl in a biodiesel/natural gas fired GT combustor. Benaissa et al. [16] demonstrated numerically that increasing swirl number leads to improved mixing between air and fuel streams due to increasing the tangential flow velocity for biogas/H_2 mixtures, with Anuj et al. [17] using simulations to show similarly that enhanced CH_4-air mixing with swirl number reduces peak temperature, and therefore NO_x.

In addition to turbulent mixing, ambient conditions are instrumental for defining the chemical kinetics of emissions formation, with contrasting trends demonstrated for different fuels – NO_x emissions from fuel blends comprising NH_3 have been shown to reduce with an increase in ambient combustor pressure [18-20]. This primarily results from augmented production of NO from OH, alongside consumption with NH and NH_2. This has been demonstrated for both premixed [18] and diffusion [20] flames, however the response is non-monotonic, as a function of NH_3-H_2 ratio. The change in stability limits and NO emissions from premixed swirling NH_3-air flames enriched with H_2/CH_4 were investigated at elevated pressure by Khateeb et al. [21]. Pressure rise was shown to widen the stability range whilst reducing NO emissions. The sensitivity to change in fuel ratio is explored in detail in this study, with the performance compared from a change in burner geometry.

Finally, Douglas et al. [22] recently quantified the potential for augmentation in emissions reporting, as a result of varying exhaust water fractions due to combustion of alternative fuels. Once dried, product NO_x concentrations were shown to be falsely inflated for H_2 blends compared with CH_4, making the traditional normalization process unsuitable for a direct comparison between fuels. In this study, product NO emissions were normalized using both traditional (dry ppm_V at 15% oxygen (O_2), as is currently used in international standards - ISO 11042 [23]) and alternative methodologies proposed in contemporary research literature [22].

2. EXPERIMENTAL FACILITY AND DIAGNOSTICS

This study was performed using a well-documented [18, 20] geometrically generic swirl burner designed and employed at Cardiff University's Gas Turbine Research Centre. The system has been employed previously in a range of configurations for the application of traditional [24, 25] and alternative fuels [26].

2.1 Pressurized Optical Combustor

The burner was employed in a non-premixed, co-annular flow configuration in this study. The assembly and pressure casing are presented schematically in cross-section in Fig. 1. The fuel injector comprises a 18 mm OD lance (Fig.1a), with a concentric 5 mm diameter plain-orifice for high velocity injection (Flow path 1) of the specified reactants. Mixtures were blended upstream of the injector from independent fuel supplies in a delivery manifold.

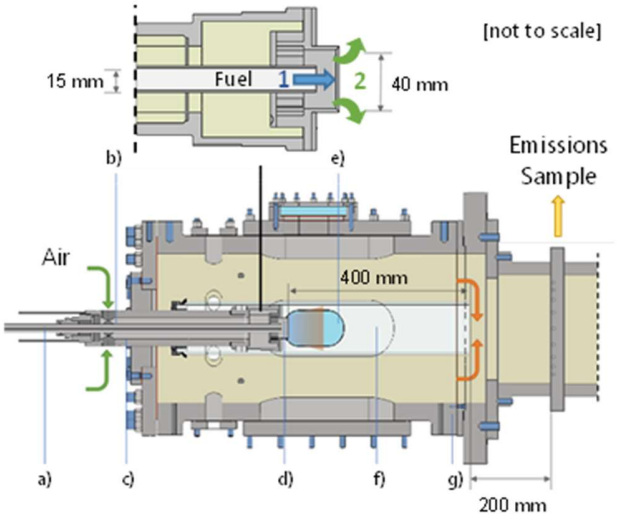

FIGURE 1: CROSS-SECTIONAL SCHEMATIC OF THE BURNER AND CASING ASSEMBLY.

Compressed air entered the burner through the inlet plenum (Fig.1b) with all fuel and air flows metered using a combination of Coriolis mass-flow controllers (±0.35%). The plenum body was preconditioned to the specified inlet temperature (T = 500 K) using preheated air, dried to a dew point of -17°C. System temperatures were allowed to stabilize for at least an hour before data were captured. The premixing chamber (Fig.1c - unused in this work) fed air to a radial-tangential swirler (Fig.1d) to envelop the injected fuel flow (flow path 2), with a burner exit nozzle radius equivalent to 20 mm. Both medium and high swirl nozzles were employed for this work (Fig. 2), with respective geometric swirl numbers equivalent to Sg = ~0.8 and Sg = ~2.0, as defined in Eqn. (1) [25]:

$$Sg = \frac{A_{noz} \cdot r_{tan}}{A_{tan} \cdot r_{noz}} \left(\frac{Q_{tan}}{Q_{total}}\right)^2 \quad (1)$$

where A_{noz} is the exit area of the burner nozzle, A_{tan} tangential inlet area, r_{tan} the effective radius of the tangential inlet, r_{noz} the nozzle radius, Q_{tan} is the tangential flow rate, and Q_{total} the total flow rate.

Quartz windows (Fig.1e) facilitated optical access into the insulated high-pressure casing (Fig.1g) with high-speed chemiluminescence measurements captured from the side, perpendicular to the reactant flow direction. The flame was housed within a cylindrical quartz confinement (Fig.1f) tube with an expansion equivalent to 100 mm from the swirler nozzle. The system was pressurized to each specified ambient condition (P) using a water-cooled incremental back-pressure valve, positioned downstream of the flame and temperature-conditioned emission sample probe. Further detail on the experimental setup is provided in other studies [18, 19, 25], with CAD models available on request.

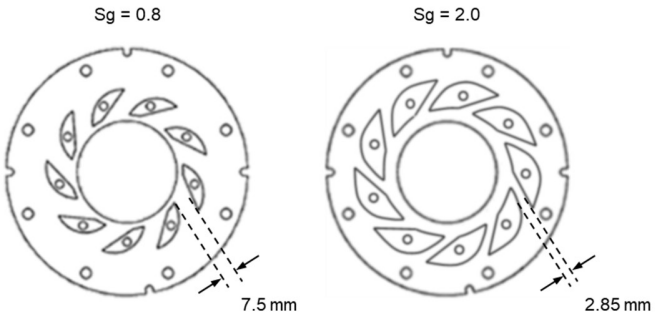

FIGURE 2: COMPARSION OF SWIRLER GEOMETRIES EMPLOYED FOR THIS WORK.

2.2 Emissions Measurement

Gaseous emissions were captured from the combustor exhaust, downstream of the quartz confinement using a 9-hole equal-area probe. The sample system was water-conditioned with a heat exchanger to regulate sample temperature to 433 K, alongside the pump, lines, and filter block following specifications in ISO-11042 [23].

NO, measurements were quantified hot/wet at 1 Hz using a heated vacuum chemiluminescence analyzer (Signal 4000VM). Additional flow was directed to a chiller, used to reduce the molar water concentration below 1% before downstream CO, CO_2 and O_2 measurements were undertaken using a combination of nondispersive infrared and paramagnetic analyzers (Signal instruments 9000MGA) respectively. Two methods of emissions normalization are compared in this work:

Normalization method 1: Dry ppm_V at 15% oxygen (O_2). Firstly, measured ppm_V concentrations (NOmeas) were corrected to equivalent dry values using Eqn. (2).

$$\text{NO Dry} = \frac{\text{NOmeas}}{1 - X_{H_2O}} \quad (2)$$

Exhaust water fractions (X_{H_2O}) were obtained from equilibrium modelling, with further detail provided in Section 3.1. Measured dry O_2 fractions (X_{O_2}) were then used to subsequently normalize readings to an equivalent reference 15% O_2 as shown in Eqn. (3) [23]

$$\text{NO Dry } 15\%\ O_2 = \text{NO Dry} \cdot \left(\frac{0.209 - 0.15}{0.209 - X_{O_2}}\right) \quad (3)$$

Normalization method 2: Here, the mass of NO produced ($\dot{m}_{NO}$) was scaled by the thermal power (q_{in}) supplied to the burner for each condition, calculated using Eqn. (4) below from Douglas et al. [22].

$$\text{NO}\ \frac{\dot{m}_{NO}}{q_{in}} = \frac{X_{NO}\ \rho_{NO}\ \dot{V}_{exhaust}}{\Delta h_c\ \rho_{fuel}\ \dot{V}_{fuel}} \quad (4)$$

Measured NO concentrations were converted to equivalent fractions (X_{NO}). Volumetric fuel flow rate ($\dot{V}_{fuel}$) was simply calculated from the specified inlet conditions, along with density. The unmeasured major components of the exhaust flow were determined using the equilibrium method as above for X_{H_2O}, and converted to mass fractions. This was scaled by the total mass flow through the system and converted for the volumetric flow of the exhaust products. For mixtures, net heat of combustion (Δh_c) was scaled by mass fraction.

After changing experimental conditions, burner temperatures, pressures, flows, and emissions were stabilized and held for a minimum of 120 measurements. Systematic uncertainties comprising analyzer specification, linearization, and span gas certification, were combined with any standard deviations in measurement to give the total uncertainty represented by the error bars shown in the plotted data.

2.3 Chemiluminescence

High-speed OH* chemiluminescence imaging was performed at each experimental condition to characterize changes in flame topology. OH* measurements focused on the well-known $A^2\Sigma+–X^2\Pi$ OH* system [27]. Data were captured using a combination of Phantom v1212 high-speed CMOS camera, Specialised Imaging SIL40HG50 high-speed image intensifier, UV lens (78 mm, f/11), and a narrow 315 nm (± 15 nm FWHM) bandpass filter. Further information on this specific high-speed imaging setup is found in other works [19].

Chemiluminescence data were captured at 4 kHz, with the image intensifier gated at 10 µs. A scaled target image gave the image resolution, equal to ~5 pixels/mm, resulting in the presented view field of 100 mm (axial y) by 50 mm (radial x). Each chemiluminescence dataset was temporally averaged from 2000 instantaneous images and filtered using a 3 × 3 pixel median filter. The averaged images were then processed using a modified Abel inversion algorithm, to provide a planar representation of the three-dimensional, flame brush, as employed previously [19, 26]. An axisymmetric comparison is shown between the averaged raw OH* chemiluminescence (Fig. 3a) and equivalent Abel transform (Fig. 3b) for an example case in Fig. 3 where the centerline of the burner nozzle is represented by x = 50 mm and flow enters from the bottom. Due to space limitations, only Abel deconvoluted half-flames are presented in this paper, with the raw dataset available from the institutional repository.

3. EXPERIMENTAL SPECIFICATION

A comprehensive experimental matrix was specified for the range of fuel mixtures, with only the salient results presented and discussed. The full experimental dataset of inlet conditions and results is available through supplemental material and the institutional repository. Experiments were performed using a swirling diffusion flame with a fixed reactant inlet temperature (T) of 500 ±10K. Air flows were specified to simulate a constant turbine inlet temperature, and therefore varied for each fuel mixture. The CHEMKIN-PRO equilibrium reactor was used to

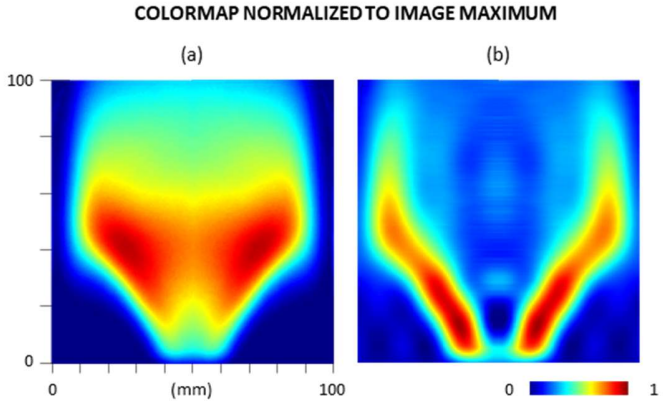

FIGURE 3: COMPARISON BETWEEN THE (a) TEMPORARILY AVERAGED RAW OH* CHEMILUMINESCENCE IMAGE AND (b) EQUIVALENT ABEL TRANSFORM.

generate adiabatic flame temperatures (AFT) for global fuel-air equivalence ratios (Φ) under conditions of constant enthalpy/pressure using the GRI-Mech 3.0 reaction mechanism [28] (53 chemical species and 325 reactions). Alternative mechanisms [29, 30] were appraised, with near negligible differences observed for AFT calculations (<0.4%). The baseline condition was defined for CH_4-air, with Φ = 0.6, giving an equivalent AFT of ~1813 K. The corresponding Φ value for each fuel was then established to give the same approximate AFT, as shown in Table 1 alongside the range of experimental P and Sg. Precisely controlled experimental mass flow rates were captured and fed back into the equilibrium reactor to provide the range of simulated AFT values represented in Table 1 for each dataset. Differences in stoichiometric airflow requirements meant that even with changing Φ, air mass flow rates and bulk outlet velocities only varied by ± 3% from the average value for all fuels at each equivalent ambient condition.

TABLE 1: SUMMARY OF EXPERIMENTAL CONDITIONS

Fuel (mol fraction)	P (MPa)	Sg	Φ	AFT (K)
1 CH_4	0.11 – 0.6	0.8, 2.0	0.6	1813 ±3
1 H_2	0.11 – 0.6	0.8, 2.0	0.503	1808 ±4
1 CH_4 ⟶ H_2 (0.2 incr.)	0.11	0.8, 2.0	0.6-0.503	1808 ±3
0.2 CH_4, 0.8 H_2	0.11 – 0.6	0.8	0.545	1807 ±2
0.25 NH_3 0.75 H_2	0.11 – 0.6	0.8, 2.0	0.546	1809 ±4
0.15 NH_3, 0.85 H_2	0.11 – 0.6	2.0	0.53	1813 ±2
0.08 NH_3, 0.92 H_2	0.11 – 0.6	2.0	0.52	1811 ±3

CH_4/H_2 ratios were initially varied in fractional increments of 0.2, however small changes were observed until an equivalent H_2 fraction of 0.8 was reached. This blend was therefore specified for further detailed testing across the full range of P.

Furthermore, after some preliminary investigation, three molar NH_3/H_2 ratios were specified at 0.25/0.75, 0.15/0.85 and 0.08/0.92, as this was predicted to adequately capture the non-monotonic influence of pressure increase on NO production with NH_3. Data were not captured for pure NH_3 flames in this work as limitations in fuel vapor withdrawal meant equivalent ambient combustor pressures could not be matched against the other fuels. A new fuel delivery system will facilitate this in future work.

To minimize differences in local velocities and combustor residence time, mass flows, and therefore net thermal powers were scaled with an increase in P at a ratio of 12.5 kW/0.11 MPa. This gave a maximum thermal power equivalent to ~68 kW at the highest-pressure condition – 0.6 MPa. Hence, whilst nozzle outlet velocities remained quasi-steady with an increase in P, Reynolds numbers (Re) and therefore local turbulence intensity increased in almost direct proportion. Taking the $\Phi = 0.6$ CH_4 case as an example, at 0.11MPa the nozzle airflow Re was ~8,500, increasing to ~46,200 at 0.6 MPa. The rise in ambient pressure also mildly increased the AFT for each specified fuel blend. This simulated change has been plotted for three example fuel mixtures (CH_4-air, H_2-air, and NH_3/H_2-air) in Fig. 4, with a near equivalent offset of ~2 K for each mix across the experimental range. The full range of calculated outlet velocities and Reynolds numbers are provided for each experimental condition in the supplemental material available through the institutional repository.

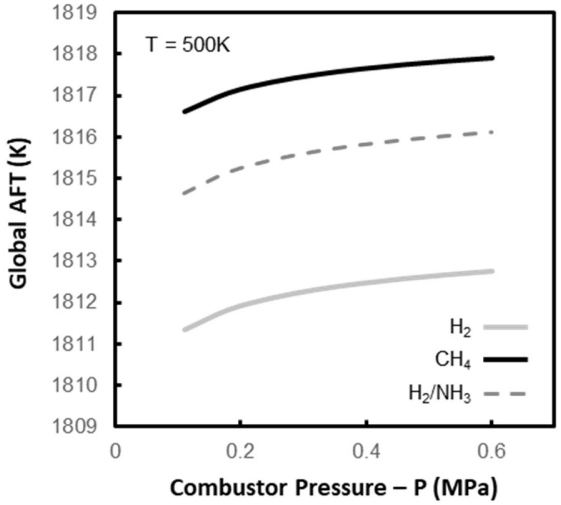

FIGURE 4: CHANGE IN GLOBAL AFT WITH P FOR CH_4 (Φ=0.6), H_2 (Φ=0.503), AND 0.25 / 0.75 NH_3/H_2 (Φ=0.548).

4. RESULTS AND DISCUSSION

4.1 CH_4 to H2

To demonstrate the change in emissions production for a variable fuel blend, H_2 fuel fraction - in CH_4- was increased in increments of 0.2. Figure 5 presents a comparison between normalized NO concentrations processed using each methodology outlined in Section 2.2 for this range in fuel composition. Initially, only a moderate increase in NO is observed, increasing considerably once the H_2 fraction is increased above 0.6, consistent with other research findings [31, 32]. This is well-understood to be a result of increased peak temperatures for the H_2 enriched flames, leading to thermal NO production.

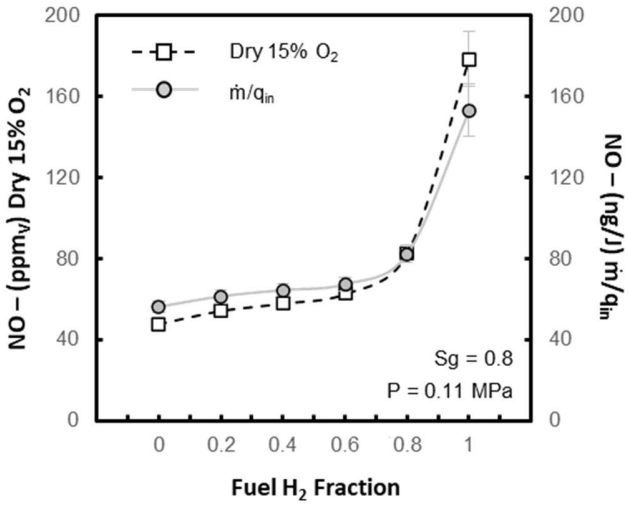

FIGURE 5: CHANGE IN NORMALIZED NO PRODUCTION FOR INCREASING MOLAR H_2 FRACTION WITH CH_4 AT 0.11 MPa.

An increase in reactivity from H_2 enrichment typically acts to shorten premixed flames, evidenced in previous studies [33]. However, the inverse effect was demonstrated with the flame configuration employed for this work, as shown in the Abel transformed OH* chemiluminescence images presented in Fig. 6. Here, the flame brush elongates from the burner face and taking OH* as a generalized marker for heat release [34], provides an increase in flame zone residence time. This results from a significant rise in the fuel injector jet velocity with H_2 enrichment; as the combined effects of density change and heating value are factored, the nozzle bulk jet velocity increases from ~30 $m \cdot s^{-1}$ for CH_4 to ~99.5 $m \cdot s^{-1}$ for H_2. This acts to reduce the strength of the central recirculation zone (CRZ) formed by the swirling airflow, as characterized for this swirler in previous studies [24]. Nevertheless, the flame still appears stabilized in the shear layer between the outward swirling bulk airflow and CRZ, resulting in the familiar V-shape flame typically associated with swirlers of this design [25, 33].

Whilst at first seeming subtle, the difference resulting from the change in normalization methodology provides a notable difference in NO emission performance. Production is shown to increase with a transition from CH_4 to H_2 by a factor of ~3.7 for the 15% dry O_2 case, versus ~2.7 from mass scaled by thermal power. This emphasizes the need to apply a suitable correction methodology to fully appraise burner performance when fuel switching.

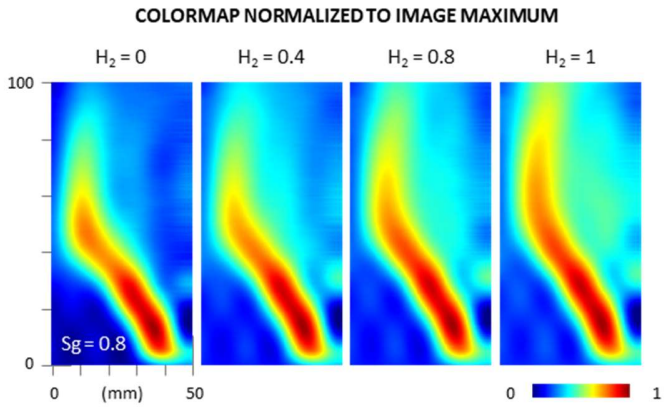

FIGURE 6: COMPARISON OF ABEL TRANSFORMED OH* CHEMILUMINESCENCE RESULTING FROM A FUEL SWITCH FROM CH_4 TO H_2 AT 0.11 MPa.

The comparative change in NO production between CH_4 and H_2 was further evaluated by increasing ambient combustor pressure. Figure 7 demonstrates this change across the full experimental range from 0.11 to 0.6 MPa, with an intermediate $0.8/0.2_{mol}$ H_2/CH_4 fuel blend, alongside a comparison between the normalization methodologies for each fuel mixture. There is near equivalent performance across the experimental range, with NO production for both CH_4 and H_2 increasing by ~70% from 0.11-0.6 MPa regardless of which normalization methodology is employed. Whilst H_2 initially shows a more prominent increase at lower pressures, production begins to plateau, as observed in other work [31], where typically NO_x emissions increase as a general square root function with increasing pressure for non-premixed flames [31]. Applying a power law correlation to these data, the pressure exponent increases marginally from the CH_4 flame (0.308) to the H2 case (0.338), demonstrating an increased sensitivity to pressure, as observed in [31].

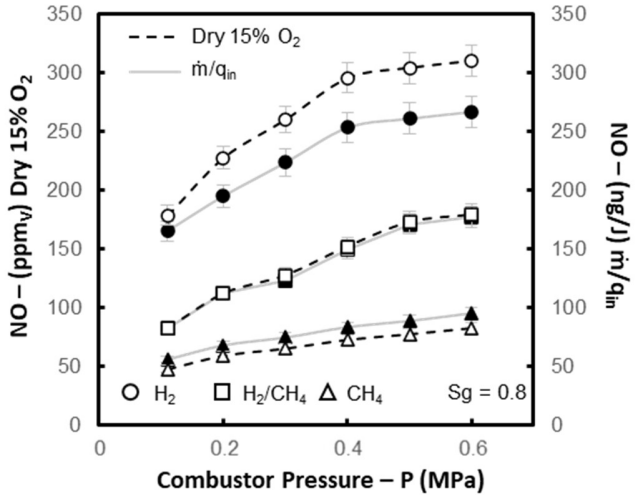

FIGURE 7: CHANGE IN NORMALIZED NO PRODUCTION FOR INCREASING AMBIENT COMBUSTOR PRESSURE, FOR CH_4, H_2 AND $0.8/0.2_{mol}$ H_2/CH_4 FUEL BLEND.

The $0.8/0.2_{mol}$ fuel blend, whilst producing lower overall emissions than the H_2 flame, demonstrates an increased sensitivity to pressure increase as NO emissions rise by over 115% at 0.6 MPa, yielding an equivalent pressure exponent of 0.458. The exponents presented were obtained using data normalized on a mass/power basis using method 2 – near equivalent exponents were observed if emissions are normalized using the traditional methodology. The $0.8/0.2_{mol}$ blend also shows minimal difference between the two emission correction methodologies, compared to the respective over/under correction given by using dry 15% dry O_2 for H_2/CH_4. Figure 8 shows the change in flame topology that results from an increase in pressure with Abel transformed OH* chemiluminescence images for the CH_4 and H_2 flames.

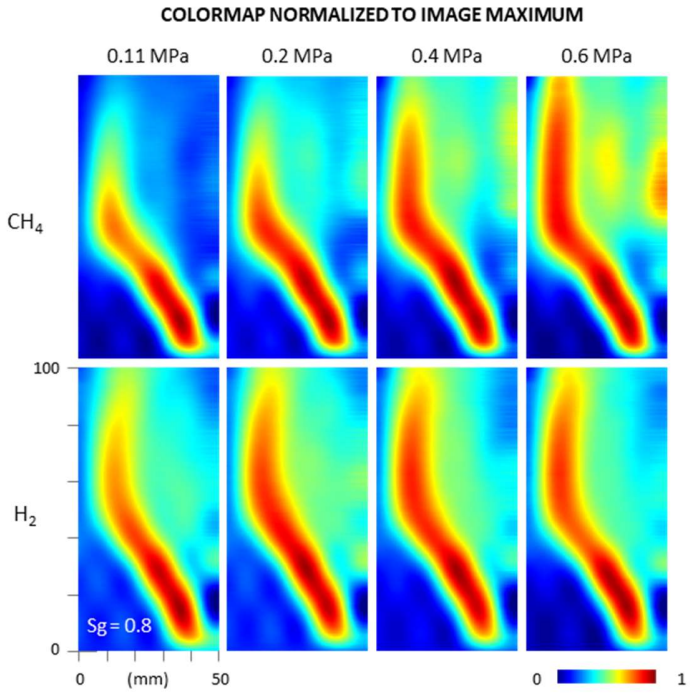

FIGURE 8: COMPARISON OF ABEL TRANSFORMED OH* CHEMILUMINESCENCE RESULTING FROM AN INCREASE IN COMBUSTOR PRESSURE FOR CH_4 AND H_2.

The CH_4 flame appears to elongate more substantially with an increase in pressure, and whilst the effect is observed for H_2 it is diminished in comparison. These trends are evident despite nozzle outlet velocities remaining quasi-constant between each condition, and near equivalent changes in Re between each fuel as pressure rises. This is attributed to a combination of change in momentum, mixing and heat release as pressure increases. As the flame elongates, this increases residence time in the flame zone, contributing to the enhanced thermal NO production, whilst post-flame NO_x production can also be exacerbated at increased pressure [35]. This is countered by the change in turbulent mixing that results from the change in density and Re. Tabet et al. [36] observed that the non-premixed H_2 flame

reaction zone becomes thicker as pressure increases, with a fast increase in peak temperature and from 1 to 5 atm reducing thereafter and reducing thermal NO production. This contributes to the plateau observed for H_2 in Fig, 7. At the highest experimental pressure condition of 0.6 MPa the switch in fuel H_2 from CH_4 results in an increase in NO production by near equivalent factors of ~3.7 (15% dry O_2) and ~2.7 (mass/thermal power) to the atmospheric case. However, prior to the plateau in NO emissions from H_2, these factors increase to maximum values of 4.1 (15% dry O_2) and 3.0 (mass/ thermal power) at 0.4 MPa.

4.2 Change in Swirl Number

Corresponding experiments were performed with both CH_4 and H_2 at high swirl conditions (Sg = 2.0), with Figure 9 highlighting the difference in measured NO between each swirler for increasing pressure. Note, for clarity only data normalized using method 2 for mass/thermal power are presented.

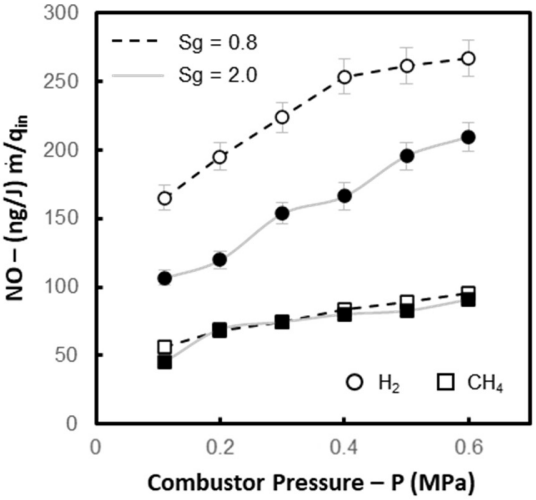

FIGURE 9: CHANGE IN NORMALIZED NO PRODUCTION FOR CH_4, AND H_2 WITH Sg AND INCREASING AMBIENT COMBUSTOR PRESSURE.

There exists a marked contrast in response to changing swirl number for each fuel: minimal differences in NO production are observed for CH_4 at each pressure, whereas notable reductions are evident for H_2 with increase in swirl number across the experimental range (max 38%). Rashwan [3] demonstrated that an increase in swirl number with CH_4 should enhance mixing, thereby lowering peak temperatures as premixed behaviour is approached. However, that effect was not observed for the CH_4 flame in this work. Oh et al. [5] demonstrated that increase in swirl vane angle improved mixing with an H_2 flame, reducing flame length and pollutant NO_x emissions, with Kim et al. [6] demonstrating equivalent trends. A comparison is made in Fig. 10 between the change in heat release and flame topology that results from an increase in Sg with Abel transformed OH* chemiluminescence images for both the CH_4 and H_2 flames.

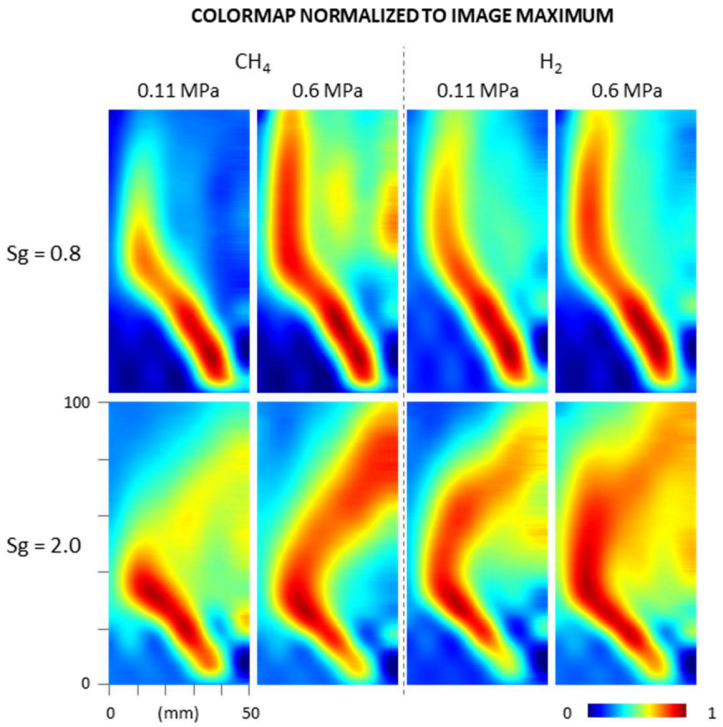

FIGURE 10: COMPARISON OF ABEL TRANSFORMED OH* CHEMILUMINESCENCE RESULTING FROM A CHANGE IN Sg, AT BOTH 0.11 AND 0.6 MPa FOR CH_4 AND H_2.

Similar trends are shown for each fuel at both elevated and low pressure – the increase tangential momentum that results from a higher Sg serves to strengthen the CRZ relative to the injection of the central fuel jet. With the flame initially stabilized in the shear layer, the overall flame length is shortened, drawing downstream reacting flow from the combustor wall. It appears the enhanced H_2 diffusivity and reduction in chemical timescales, supported by the improved mixing from increased Sg, limits peak temperatures, therefore facilitating a drop in NO production. Whilst overall NO concentrations for H_2 are lower for Sg = 2.0 than 0.8, the increase that results from a rise in combustor pressure is more pronounced, with the relative plateau observed for Sg = 0.8 diminished with an equivalent pressure exponent of 0.411, suggesting increased sensitivity. NO concentrations almost double (compared to an increase of ~70%) for this blend across the experimental range. Nevertheless, there is still a marked improvement in the emissions produced from the H_2 flame compared to CH_4, where the pressure exponent also increased to 0.386, with NO only increasing by a factor of 1.7-2.3 (mass/ thermal power) for the pressure range considered.

Contrasting behavior was observed once the burner was fueled with a 0.75/0.25$_{mol}$ H_2/NH_3 blend. Figure 11 provides a comparison in trends for NO emissions for each Sg with an increase in ambient pressure across the specified range. Once again, a comparison is made between each method of emissions normalization, with a small offset between each case.

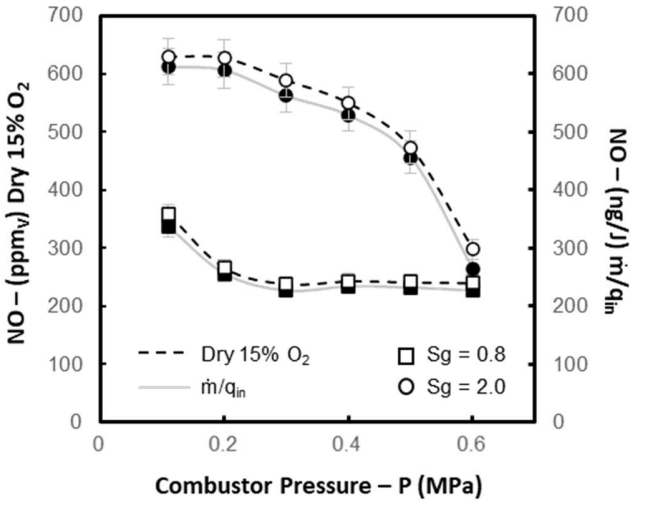

FIGURE 11: CHANGE IN NORMALIZED NO PRODUCTION FOR 0.75/0.25 H_2/NH_3 WITH Sg AND INCREASING AMBIENT COMBUSTOR PRESSURE.

Non-premixed NH_3 and H_2/NH_3 flames have previously been shown to generate a reduction in NO for an increase in pressure [18-20], however the profiles evident in Fig. 11 change markedly with a switch in swirl number. For the Sg = 0.8 case, NO quickly falls to values lower than measurements made with pure H_2 flames at P = 0.6 MPa. However, a relative plateau is reached, and the emissions do not fall once P = 0.3 MPa is exceeded. This behavior with increase in pressure has been observed for premixed flames and is attributed to enhanced consumption of NO with NH and NH_2 alongside reduced production from the reaction: HNO + OH ↔ NO + H_2O. A reduction with increasing pressure is also observed for the Sg = 2.0 condition, however the inverse trend is evident, where the reduction in NO emissions appears to be increasingly enhanced as pressure is increased. Figure 12 provides a comparison between Abel transformed OH* chemiluminescence for each swirl number with this fuel blend. Once again, similar behavior is evident for the CH_4 and H_2 flames – at Sg = 0.8, the flame is stabilized along the shear layer, with a traditional V-shape, similar to a premixed configuration. However, once Sg is increased to 2.0, the strengthened CRZ appears to draw more reacting flow from the combustor wall. A potential explanation for the observed trend in emissions is that for the high swirl case, more reacting flow is being directed to where the flame is richest. Pressure increase has been shown to provide an increase in NH_2 production, which would act to consume NO formed in the shear layer. Recent work by Wang et al. [37] demonstrated that for a premixed flame, using swirl number to increase residence time reduced NO, N_2O and NO_2 emissions more efficiently than tripling the chamber's length. However, this may be partly attributed to a decrease in combustion efficiency. Interestingly, the study by Wang et al. [37] was performed at a fixed P = 0.2 MPa, and at that single pressure the opposite trend is witnessed to that observed in this work – that is, markedly worse NO_x performance for the high swirl case (NO fractions more than doubled at Sg = 2.0), and convergence only observed at the highest pressure conditions. Regarding combustion efficiency, no marked reduction was evident throughout this work. A comparison between the NH_3/H_2, CH_4 and H_2 exhaust temperatures – measured using an R-type thermocouple positioned downstream of the quartz tube (Fig. 1f) – are shown in Fig. 13, alongside the measured differences in exhaust O_2 for NH_3/H_2 across the pressure range. Whilst no substantial efficiency drop is evident, the potential exists for enhanced trace NH_3 slip, as would be expected with enhanced NH_2 production [18]. For this work NH_3 data could not be accurately measured, however it is not unreasonable to suggest that a small increase in NH_3 slip would result given the observed NO reductions, and previous work [18, 19, 37]. Additional research is required to evaluate how the trends observed would continue with further rise in combustor pressure. Nevertheless, results suggest that high swirl is favorable with non-premixed flames for fuels comprising NH_3 at significantly elevated pressure.

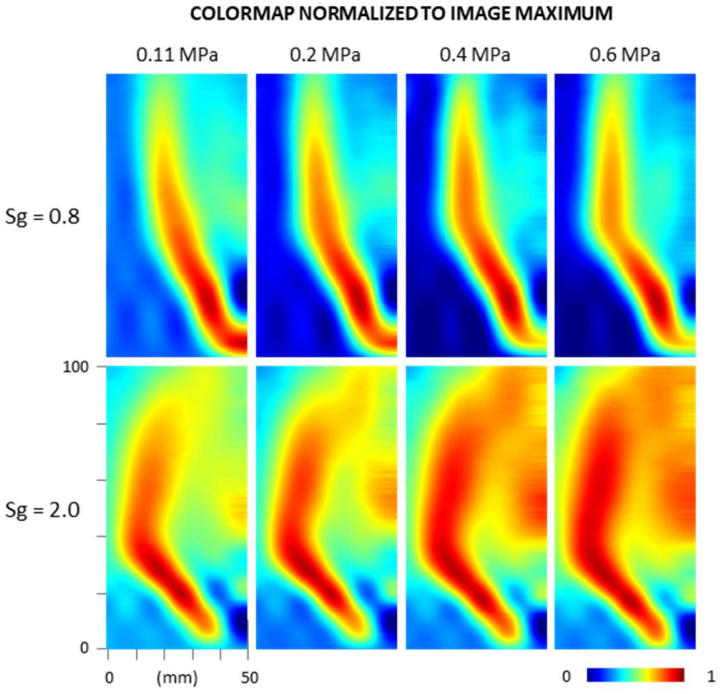

FIGURE 12: COMPARISON OF ABEL TRANSFORMED OH* CHEMILUMINESCENCE RESULTING FROM A CHANGE IN Sg FOR 0.75/0.25$_{mol}$ H_2/NH_3 ACROSS THE CHANGE IN P.

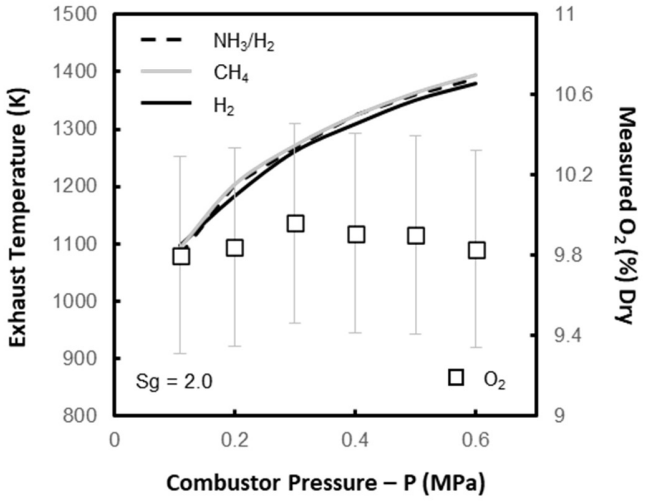

FIGURE 13: COMPARISON OF THE DIFFERENCES IN MEASURED EXHAUST TEMPERATURES FOR NH_3/H_2, CH_4 AND H_2 AT Sg = 2.0, WITH CHANGE IN O_2 FROM THE NH_3/H_2 FLAME.

4.3 change in NH_3/H_2 ratio

Two additional ratios of H_2/NH_3 ($0.85/0.15_{mol}$, and $0.92/0.08_{mol}$) were specified to characterize the sensitivity in reducing NO with pressure. The aim was to identify the approximate NH_3 concentration necessary for the beneficial influence of increasing pressure to be realized. The change in measured exhaust NO between each fuel blend is shown in Fig. 14. Again, data are presented normalized only using method 2 for mass/thermal power for clarity.

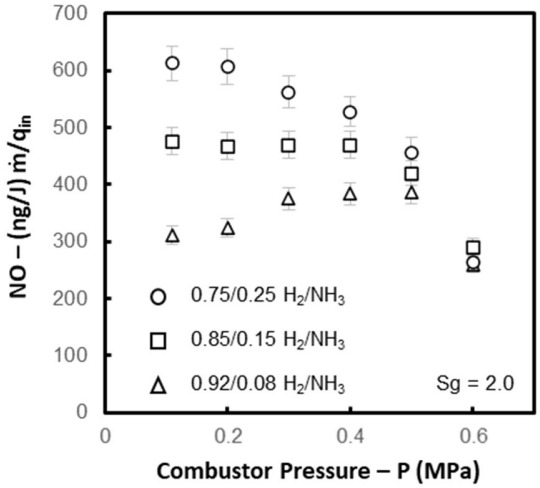

FIGURE 14: CHANGE IN NORMALIZED NO PRODUCTION FOR THREE H_2/NH_3 BLENDS WITH INCREASING AMBIENT COMBUSTOR PRESSURE.

Opposing trends were observed between each blend as combustor pressure increased. The $0.92/0.08_{mol}$ H_2/NH_3 ratio provided an increasing trend similar to the CH_4, H_2 and H_2/CH_4 experiments, however with a reduced rate of increase. This contrasts with the $0.75/0.25_{mol}$ H_2/NH_3 where a growing reduction was previously observed in Section 4.2. The $0.85/0.15_{mol}$ H_2/NH_3 mostly provides a relative plateau in NO, and marks approximately the ratio at which the beneficial impact of increasing pressure up to 0.4 MPa on NO production is achieved with this burner configuration. However, at the highest pressure condition (P = 0.6 MPa), a reduction in NO is evident for all applied fuel ratios, and presents a point of convergence for each mixture. This is noteworthy, as no distinct change in flame topology was evident, as shown in Fig. 15 with averaged Abel transformed OH* chemiluminescence.

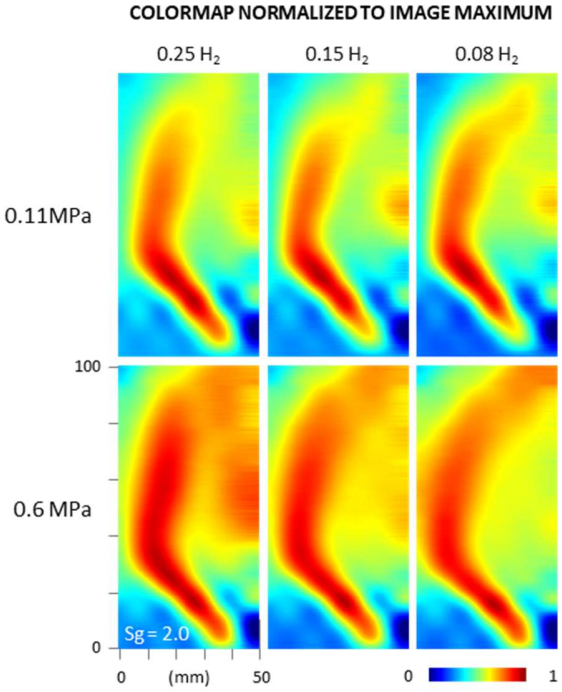

FIGURE 15: COMPARISON OF ABEL TRANSFORMED OH* CHEMILUMINESCENCE RESULTING FROM A CHANGE IN H_2/NH_3 RATIO ACROSS THE CHANGE IN P.

The relative reduction in H_2 fraction provides a small increase in flame length at each pressure, with a more pronounced lengthening as the maximum pressure is achieved. However, the same overall flame shape is maintained, again with downstream reacting flow being drawn in from the combustor wall. There was an increase in bulk injector outlet velocity from ~92 to ~97 $m \cdot s^{-1}$ as molar NH_3 fraction reduced from 0.25 to 0.08. However, this was near equivalent to the pure H_2 case, and considerably higher than the CH_4 condition. The chemiluminescence data suggests the enhanced recirculation resulting from high swirl is controlling the flow structure to give a near equivalent flame topology for all fuels.

Whilst the emissions convergence at P = 0.6 MPa requires further study, it should be noted that for the NH_3/H_2 blends used in this work, emissions performance observed at the highest pressure condition approaches that of the pure H_2 flame.

Furthermore, at the Sg = 0.8 condition, better performance is demonstrated for the $0.75/0.25_{mol}$ H_2/NH_3 mixture relative to H_2 once P = 0.3 MPa is exceeded. The potential exists for these trends to continue with a further increase in ambient combustor pressure.

5. CONCLUSIONS

To conclude, an experimental study was performed to appraise the comparative emissions performance of a non-premixed, co-annular swirl burner supplied with CH_4 NH_3, and H_2 in different mixture ratios. The influence of change in swirl number and combustor ambient pressure were quantified.

A fuel switch from CH_4 to H_2 provided an increase in NO production, with measured concentrations rising rapidly once molar fractions of 0.6 were exceeded, consistent with previous work. A rise in ambient combustor pressure leads to an increase in NO production with both fuels and intermediate blends, and attention must be given to the emissions normalization methodology adopted when appraising the relative performance with a fuel switch.

An increase from medium to high radial-tangential swirl (corresponding to geometric swirl numbers of 0.8 and 2.0) provided no significant change in NO emissions production for the CH_4 flame. However, significant reductions were observed for the non-premixed H_2 flame across all experimental combustor pressures, reaching a maximum of 38%. Results are discussed in relation to changes in flame topology, visualized using high-speed OH* chemiluminescence.

A marked difference in NO production with increasing pressure was observed if a molar H_2/NH_3 ratio of 0.75/0.25 is employed. At medium swirl, NO concentrations drop rapidly and reach a relative plateau that outperforms pure H_2 at the highest pressure conditions. At high swirl, NO fractions continue to decrease as combustor pressure is raised, with no observable change in combustor efficiency across the evaluated range.

Finally, the molar H_2/NH_3 ratio was varied to investigate the blend at which the beneficial impact of pressure increase on NO reduction is no longer realized. Results suggest this is near the H_2/NH_3 ratio of $0.85/0.15_{mol}$. Emissions performance converged as the maximum pressure investigated was approached, and a decrease in NO was still measured for all fuel blends up to 0.6 MPa, beyond which further investigation is required.

ACKNOWLEDGEMENTS

This project has received funding from the European Union's Horizon 2020 research and innovation programme under grant agreement N° 884157, alongside IDRIC (Industrial Decarbonised Research and Innovation Centre, EP/VO27050/1, Project 40) The research was undertaken at the Cardiff University's GTRC with invaluable technical support from Jack Thomas.

SUPPLEMENTARY MATERIAL

Supplementary material associated with this article can be found, in the online version, at: https://www.cu-gtrc.co.uk/

REFERENCES

[1] IPCC, 2014: Climate Change 2014: Synthesis Report. Contribution of Working Groups I, II and III to the Fifth Assessment Report of the Intergovernmental Panel on Climate Change IPCC, 151.

[2] Lieuwen, Timothy, McDonell, Vince, Petersen, Eric, and Santavicca, Dominic. "Fuel Flexibility Influences on Premixed Combustor Blowout, Flashback, Autoignition, and Stability". *Journal of Engineering for Gas Turbines and Power* (2008) Vol. 130 https://doi.org/10.1115/1.2771243

[3] Rashwan, Sherif S. "The Effect of Swirl Number and Oxidizer Composition on Combustion Characteristics of Non-Premixed Methane Flames" *Energy & Fuels* Vol. 32 (2018), pp. 2517-2526 https://doi.org/10.1021/acs.energyfuels.8b00233

[4] Yılmaz, İlker "Effect of Swirl Number on Combustion Characteristics in a Natural Gas Diffusion Flame" *ASME Journal of Energy Resources. Technology* Vol. 135 (2013) 042204. https://doi.org/10.1115/1.4024222

[5] Oh, Jeongseog, Hwang, Jeongjae, Yoon, Youngbin, "EINOx scaling in a non-premixed turbulent hydrogen jet with swirled coaxial air" *International Journal of Hydrogen Energy* Vol. 35 (2010) pp. 8715-8722. https://doi.org/10.1016/j.ijhydene.2010.04.159.

[6] Kim, Han, Arghode, Vaibhav, Linck, Martin, and Gupta, Ashwani "Hydrogen addition effects in a confined swirl-stabilized methane-air flame" *International Journal of Hydrogen Energy* Vol. 34 (2009) pp. 1054-1062. https://doi.org/10.1016/j.ijhydene.2008.10.034

[7] Gupta, Ashwani, Lewis, M. and Daurer, M. Swirl Effects on Combustion Characteristics of Premixed Flames" *Journal for Engineering Gas Turbines and Power* Vol. 123 (2001): pp. 619–626. https://doi.org/10.1115/1.1339987

[8] Kashir, Babak, Tabejamaat, Sadegh, Jalalatian, and Nafiseh, "A numerical study on combustion characteristics of blended methane-hydrogen bluff-body stabilized swirl diffusion flames" *International Journal of Hydrogen Energy* Vol. 44 (2015) pp. 6243-6258 https://doi.org/10.1016/j.ijhydene.2015.03.023

[9] De, Ashoke, Acharya, Sumanta, "Parametric study of upstream flame propagation in hydrogen-enriched premixed combustion: Effects of swirl, geometry and premixedness" *International Journal of Hydrogen Energy* Vol. 37 pp. 14649-14668. https://doi.org/10.1016/j.ijhydene.2012.07.008

[10] İlbaş, Mustafa, Karyeyen, Serhat, Yilmaz, İlker, "Effect of swirl number on combustion characteristics of hydrogen-containing fuels in a combustor" *International Journal of Hydrogen Energy* Vol. 41 pp. 7185-7191 https://doi.org/10.1016/j.ijhydene.2015.12.107

[11] Khalil, Ahmed, Gupta, Ashwani K, "Swirling distributed combustion for clean energy conversion in gas turbine applications" *Applied Energy* Vol. 88 (2011) pp.3685-3693, https://doi.org/10.1016/j.apenergy.2011.03.048

[12] Patel, Vipul, and Shah, Rupesh "Effect of hydrogen enrichment on combustion characteristics of methane swirling and non-swirling inverse diffusion flame" *International Journal of Hydrogen Energy* Vol. 44 pp. 28316-28329 https://doi.org/10.1016/j.ijhydene.2019.09.076

[13] Jalalatian, Nafiseh, Tabejamaat, Sadegh, Kashir, Babak and Eidi Attar Zadeh, Masoud. "An experimental study on the effect of swirl number on pollutant formation in propane bluff-body stabilized swirl diffusion flames" *Physics of Fluids* Vol. 31 (2019) https://doi.org/10.1063/1.5110505

[14] Mansouri, Zakaria, Aouissi, Mokhtar, and Boushaki, Toufik "Numerical computations of premixed propane flame in a swirl-stabilized burner: Effects of hydrogen enrichment, swirl number and equivalence ratio on flame characteristics" *International Journal of Hydrogen Energy* Vol. 41 pp. 9664-9678 https://doi.org/10.1016/j.ijhydene.2016.04.023

[15] Chiong, Meng-Choung, Valera-Medina, Agustin Chong, William, Chong, Cheng, Mong, Guo, and Jaafar, Mohammad "Effects of swirler vane angle on palm biodiesel/natural gas combustion in swirl-stabilised gas turbine combustor" *Fuel* Vol. 277 https://doi.org/10.1016/j.fuel.2020.118213

[16] Benaissa, Sabrina, Adouane, Belkacem, Ali, S.M. and Mohammad, Akram. "Effect of hydrogen addition on the combustion characteristics of premixed biogas/hydrogen-air mixtures" *International Journal of Hydrogen Energy*, Vol. 46, (2021) pp. 18661-18677 https://doi.org/10.1016/j.ijhydene.2021.02.225

[17] Anuj B, G Mahesh Nayak, Yogesh B, and Saravanan B. "Numerical Investigation Into the Effect of Air Swirl on Non-Premixed Combustion" *ASME 2021 Gas Turbine India Conference* V001T03A002 (2021) https://doi.org/10.1115/GTINDIA2021-76016

[18] Pugh, Daniel, Bowen Philip, Valera-Medina, Agustin, Giles, Anthony, Runyon, Jon and Marsh, Richard. "Influence of steam addition and elevated ambient conditions on NOx reduction in a staged premixed swirling NH_3/H_2 flame.", *Proceedings of the combustion institute* Vol. 37 (4) (2019): pp. 5401-5409 https://doi.org/10.1016/j.proci.2018.07.091

[19] Pugh, Daniel, Runyon, Jon, Bowen, Philip, Giles, Anthony, Valera-Medina, Agustin, Marsh, Richard, Goktepe, Burak and Hewlett, Sally. "An investigation of ammonia primary flame combustor concepts for emissions reduction with OH ∗, NH_2∗ and NH∗ chemiluminescence at elevated conditions." *Proceedings of the combustion institute* Vol. 38 (4) (2021) pp. 6451-6459. http://dx.doi.org/10.1016/j.proci.2020.06.310

[20] Hayakawa, Akihiro, Goto, Takashi, Mimoto, Rentaro, Arakawa, Yoshiyuki, Kudo, Taku, Kobayashi, Hideaki. "Laminar burning velocity and Markstein length of ammonia/air premixed flames at various pressures." *Fuel* Vol. 159 (2015) pp. 98-106. https://doi.org/10.1016/j.fuel.2015.06.070

[21] Khateeb, Abdulrahman, Guiberti, Thibault, Wang, Guoqing Boyette, Wesley, Younes, Mourad, Jamal, Aqil, Roberts, William "Stability limits and NO emissions of premixed swirl ammonia-air flames enriched with hydrogen or methane at elevated pressures" *International Journal of Hydrogen Energy* Vol.46 (2021) pp. 11969-11981 https://doi.org/10.1016/j.ijhydene.2021.01.036

[22] Douglas, Christopher M. Shaw, Stephanie L. Martz, Thomas D. Steele, Robert C. Noble, David R. Emerson, Benjamin L.and Lieuwen Timothy C. "Pollutant Emissions Reporting and Performance Considerations for Hydrogen–Hydrocarbon Fuels in Gas Turbines" *Journal for Engineering Gas Turbines and Power* Vol. 144 (9) (2022) https://doi.org/10.1115/1.4054949

[23] British Standard ISO 11042-1:1996 Gas Turbines. Exhaust Gas Emission Measurement and Evaluation British Standards Institution, U.K (1996).

[24] Runyon, Jon, Giles, Anthony, Marsh, Richard, Pugh, Daniel, Goktepe, Burak, Bowen, Philip, and Morris Steven "Characterization of Additive Layer Manufacturing Swirl Burner Surface Roughness and Its Effects on Flame Stability Using High-Speed Diagnostics" *Journal for Engineering Gas Turbines and Power* Vol. 142 (9) (2020) https://doi.org/10.1115/1.4044950

[25] Runyon, Jon, Marsh, Richard, Bowen, Philip, Pugh, Daniel, Giles, Anthony, Morris, Steven, "Lean methane flame stability in a premixed generic swirl burner: Isothermal flow and atmospheric combustion characterization" *Experimental Thermal and Fluid Science*, Vol. 92 (2018) pp. 125-140 https://doi.org/10.1016/j.expthermflusci.2017.11.019.

[26] Pugh, Daniel, Valera-Medina, Agustin, Bowen, Philip, Giles, Anthony, Goktepe, Burak, Runyon, Jon, Morris, Steven, Hewlett, Sally, and Marsh, Richard. "Emissions Performance of Staged Premixed and Diffusion Combustor Concepts for an NH_3/Air Flame with and without reactant humidification." *Journal for Engineering Gas Turbines and Power* Vol. 143 (5) (2021) 051012. https://doi.org/10.1115/1.4049451

[27] A.G. Gaydon, "The Spectroscopy of Flames" (2nd Edition), Chapman and Hall, London U.K. (1974). ISBN: 978-94-009-5720-6

[28] Smith, Gregory P. Golden, David M. Frenklach, Michael, Moriarty Nigel W. Eiteneer, Boris, Goldenberg, Mikhail, Bowman, C. Thomas, Hanson, Ronald K. Song, Soonho Gardiner, William C. V. Lissianski, Vitali and Qin Zhiwei http://combustion.berkeley.edu/gri-mech/

[29] Okafor, Ekenechukwu, Naito, Yuji, Colson, Sophie, Ichikawa, Akinori, Kudo, Taku, Hayakawa, Akihiro, and Kobayashi, Hideaki. "Experimental and numerical study of the laminar burning velocity of CH_4–NH_3–air premixed flames." *Combustion and Flame* Vol. 187 (2018) pp. 185-198. https://doi.org/10.1016/j.combustflame.2017.09.002

[30] Davis, Scott G. Joshi, Ameya.V. Wang, Hai and Egolfopoulos, Fokion "An optimized kinetic model of H2/CO combustion" *Proceedings of the combustion institute* Vol. 30 (2005), pp. 1283-1292 https://doi.org/10.1016/j.proci.2004.08.252

[31] Kroninger, Daniel Prediction of NOx Emissions for a Hydrogen Fueled Industrial Gas Turbine Combustor with Water Injection. PhD thesis https://d-nb.info/1192308662/34

[32] Cellek, Mehmet Salih, and Pınarbaşı, Ali, "Investigations on performance and emission characteristics of an industrial low swirl burner while burning natural gas, methane, hydrogen-enriched natural gas and hydrogen as fuels" International Journal of Hydrogen Energy Vol. 43 (2018) pp. 1194-1207 https://doi.org/10.1016/j.ijhydene.2017.05.107.

[33] Schefer, R.W. Wicksall, D.M. Agrawal, A.K. "Combustion of hydrogen-enriched methane in a lean premixed swirl-stabilized burner" *Proceedings of the Combustion Institute* Vol. 29 (2002) pp. 843-851, https://doi.org/10.1016/S1540-7489(02)80108-0.

[34] Panoutsos, C.S. Hardalupas, Y. Taylor, Alex "Numerical evaluation of equivalence ratio measurement using OH∗ and CH∗ chemiluminescence in premixed and non-premixed methane–air flames" *Combustion and Flame,* Vol. 156 (2009) pp. 273-291 https://doi.org/10.1016/j.combustflame.2008.11.008.

[35] Biagioli, Fernando, and Güthe, Felix. "Effect of pressure and fuel–air unmixedness on NOx emissions from industrial gas turbine burners" *Combustion and Flame* Vol. 151 (2007) pp. 274-288, https://doi.org/10.1016/j.combustflame.2007.04.007

[36] Tabet, F. Sarh, B. Gökalp, I. "Turbulent non-premixed hydrogen-air flame structure in the pressure range of 1–10 atm" *International Journal of Hydrogen Energy,* Vol. 36 (2011) pp. 15838-15850 https://doi.org/10.1016/j.ijhydene.2011.08.064.

[37] Wang, Guoqing, Guiberti, Thibault F. Cardona, Santiago, Avila Jimenez, Cristian and Roberts, William L. "Effects of residence time on the NOx emissions of premixed ammonia-methane-air swirling flames at elevated pressure" *Proceedings of the Combustion Institute (2022)* https://doi.org/10.1016/j.proci.2022.07.141.

Table Caption List

TABLE 1: Summary of experimental conditions

Figure Caption List

FIGURE 1: Cross-sectional schematic of the burner and casing assembly.

FIGURE 2: Comparison of swirler geometries employed for this work.

FIGURE 3: Comparison between the (a) temporarily averaged raw OH* chemiluminescence image and (b) equivalent Abel transform.

FIGURE 4: Change in global AFT with P for CH_4 (Φ=0.6), H_2 (Φ=0.503), and 0.25 / 0.75 NH_3/H_2 (Φ=0.548).

FIGURE 5: Change in normalized NO production for increasing molar H_2 fraction with CH_4 at 0.11 MPa.

FIGURE 6: Comparison of Abel transformed OH* chemiluminescence resulting from a fuel switch from CH_4 to H_2 at 0.11 MPa.

FIGURE 7: Change in normalized NO production for increasing ambient combustor pressure, for CH_4, H_2 and $0.8/0.2_{mol}$ H_2/CH_4 fuel blend.

FIGURE 8: Comparison of Abel transformed OH* chemiluminescence resulting from an increase in combustor pressure for CH_4 and H_2.

FIGURE 9: Change in normalized NO production for CH_4, and H_2 with Sg and increasing ambient combustor pressure.

FIGURE 10: Comparison of Abel transformed OH* chemiluminescence resulting from a change in Sg, at both 0.11 and 0.6 MPa for CH_4 and H_2.

FIGURE 11: Change in normalized NO production for 0.75/0.25 H_2/NH_3 with Sg and increasing ambient combustor pressure.

FIGURE 12: Comparison of Abel transformed OH* chemiluminescence resulting from a change in Sg for $0.75/0.25_{mol}$ H_2/NH_3 across the change in P.

FIGURE 13: Comparison of the differences in measured exhaust temperatures for NH_3/H_2, CH_4 and H_2 at sg = 2.0, with change in O_2 from the NH_3/H_2 flame.

FIGURE 14: Change in normalized NO production for three H_2/NH_3 blends with increasing ambient combustor pressure.

FIGURE 15: Comparison of Abel transformed OH* chemiluminescence resulting from a change in H_2/NH_3 ratio across the change in P.